Available online at www.sciencedirect.com
SCIENCE DIRECT
Neuroscience Research 54 (2006) 202–212
Neuroscience Research
www.elsevier.com/locate/neures

Microglia/macrophages responses to kainate-induced injury in the rat retina

Min-Lin Chang [a], Ching-Hsiang Wu [b], Hsiung-Fen Chien [c], Ya-Fen Jiang-Shieh [d], Jeng-Yung Shieh [a], Chen-Yuan Wen [a,*]

[a] *Department of Anatomy and Cell Biology, College of Medicine, National Taiwan University, 1, Section 1, Jen Ai Road, Taipei 100, Taiwan*
[b] *Department of Biology and Anatomy, National Defense Medical Center, Taipei 114, Taiwan*
[c] *Department of Surgery, College of Medicine, National Taiwan University, Taipei 100, Taiwan*
[d] *Department of Anatomy, College of Medicine, National Cheng Kung University, Tainan 701, Taiwan*

Received 30 June 2005; accepted 29 November 2005
Available online 3 February 2006

Abstract

The present study was aimed to elucidate how retinal microglia/macrophages would respond to neuronal death after intravitreal kainate injection. An increased expression of the complement receptor type 3 (CR3) and an induction of the major histocompatibility complex (MHC) class II and ED-1 antigens were mainly observed in the inner retina after kainate injection. Prominent cell death revealed by Fluoro Jade B (FJB) staining and ultrastructural examination appeared at the inner border of the inner nuclear layer (INL) at 1 day post-injection. Interestingly, some immunoreactive cells appeared at the outer segment of photoreceptor layer (OSPRL) at different time intervals. Our quantitative analysis further showed that CR3 immunoreactivity was drastically increased peaking at 7 days but subsided thereafter. MHC class II and ED-1 immunoreactivities showed a moderate but steady increase peaking at 3 days and declined thereafter. Double labeling study further revealed that retinal microglia/macrophages expressed concurrently CR3 and ED-1 antigens ($OX\text{-}42^{+}/ED\text{-}1^{+}$) or MHC class II molecules ($OX\text{-}42^{+}/OX\text{-}6^{+}$) and remained branched in shape at early stage of kainate challenge. By electron microscopy, microglia/macrophages with CR3 immunoreactivity displayed abundant cytoplasm containing a few vesicles and phagosomes. Other cells ultrastructurally similar to Müller cells or astrocytes could also engulf exogenous substances. In conclusion, retinal microglia/macrophages responded vigorously to kainate-induced neuronal cell death that may also trigger the recruitment of macrophages from neighboring tissues and induce the phagocytotic activity of cells other than retinal microglia/macrophages.

Keywords: Intravitreal injection; Kainate; Microglia/macrophages; Retina

1. Introduction

The microglial cells were one of the constituent glial cell types in the retina and thought to be related to the mononuclear phagocytic system (Ogden, 1994). The retinal microglial cells, often branched, were characterized by an oval cell body bearing an elongated nucleus (Ogden, 1994). Previous studies have reported that the retinal microglia in rabbits and rats were mainly located in the nerve fiber layer (NFL), the inner plexiform layer (IPL) and, occasionally, in the outer plexiform layer (OPL) (Wang et al., 1996). The cells were believed to serve as the intrinsic immunocompetent cells in the retinal tissues (Matsubara et al., 1999) and may participate in antigen presentation, especially when they were exposed to IFN-γ (Zhang et al., 1997; Matsubara et al., 1999). They were also activated in different retinal injuries such as excitotoxic neurodegeneration (Zeevalk et al., 1989) due to excessive accumulation of glutamate (Vorwerk et al., 2000). High levels of extracellular glutamate were probably associated with the degeneration of photoreceptor cells, ischemic retina and glaucoma (Ulshafer et al., 1990; Dreyer et al., 1996; Tamai et al., 1997).

A conformationally restricted analog of glutamate viz. kainate has also been reported to have potent excitotoxicity on neurons in the hippocampus and the retina (Kleinschmidt et al., 1986). In the retina, kainate destroyed the ganglion cells leading to severe morphological changes in the IPL and the

* Corresponding author. Tel.: +886 2 3562211; fax: +886 2 3915292.
E-mail address: wency@ntu.edu.tw (C.-Y. Wen).

0168-0102/$ – see front matter
doi:10.1016/j.neures.2005.11.010

inner nuclear layer (INL) (Honjo et al., 2000). Along with the neuronal cell death induced by kainate, the retinal glial cells exhibited signs of reactive changes (Dreyfus et al., 1998). In this situation, the Müller cells were induced to show phosphoinositide hydrolysis (Lopez-Colome et al., 1993) and upregulated expression of glial fibrillary acidic protein (Honjo et al., 2000). Furthermore, retinal microglial cells as revealed by RCA-1 histochemistry were activated and followed a distribution pattern similar to the terminal transferase-mediated dUTP nick-end-labeling staining (Shin et al., 2000). Hence, it was concluded that microglia were the only phagocyte involved in kainate-induced retinal apoptosis (Shin et al., 2000). In the light of this finding and in order to gain further insights on the effect of kainate on retinal neurons, a better understanding of microglia/macrophages reaction is vital, especially in regard to the time and spatial patterns of the glial type. Indeed, the changes of immunomolecules associated with the reactive retinal microglia/macrophages have remained to be explored. Using a panel of antibodies and ultrastructural examination, this study sought to investigate thoroughly and quantitatively the time and spatial patterns in the changes of immunoexpression of the complement receptor type 3 (CR3), major histocompatibility complex (MHC) class II, and lysosome antigens in the retinal microglia/macrophages, marked by OX-42, OX-6 and ED-1, respectively, following the treatment of kainate. Results of the present study may provide insight into the relationship between the structural changes of retinas and glial activation as well as some clues for rescuing neuronal death in ischemic retinas or glaucoma suffering from a high level of neurocytotoxic glutamate.

2. Materials and methods

2.1. Tissue processing

Adult male Wistar rats weighting 250–350 g (approximately 8–10 weeks old; $n = 60$) were used in this study. All experiments were conducted in accordance with the standards of the Association for Research in Vision and Ophthalmology. Kainic acid (KA; Sigma, K0250) was dissolved in sterile normal saline solution administered at the concentration of 5 nM. Each rat was given with an intravitreal injection of 1.4 μl KA into the right eye. The same volume of sterile 0.9% normal saline was injected into the left eye as the controls. The experimental animals were sacrificed at 1, 3, 7, 14 and 28 days after injections. Eight rats were used for each time point (including untreated group). Following deep anesthesia with an intraperitoneal injection of 7% chloral hydrate, all rats were perfused with Ringer's solution, followed by 4% paraformaldehyde in 0.1 M phosphate buffer (PB; pH 7.4). After fixation, the eyeballs were removed and then the lens were detached before transferred into 30% sucrose solution and kept in the same solution overnight at 4 °C. Each eyeball was cut into sagittal sections in a cryostat at the thickness of 12 μm and the frozen sections obtained from different experimental groups were mounted on micro slides (DAKO; 5116).

2.2. Immunohistochemistry

Mounted sections were washed in Tris buffer solution (TBS) and treated in a solution containing 10% methanol and 1% hydrogen peroxide in TBS for 1 h to remove possible endogenous peroxidase and to improve the permeability of the cell membrane. After TBS washing, sections were blocked in a combination of 0.1% Triton X-100 and 10% normal horse serum (NHS) for 1 h. They were then incubated overnight with the following primary antibodies: monoclonal antibody OX-42 (1:100; Serotec, MCA275R) for the detection of CR3, monoclonal antibody OX-6 (1:400; Serotec, MCA46R) for MHC class II antigen, and monoclonal antibody ED-1 (1:100; Serotec, MCA341R) for lysosomal protein of macrophages. After incubation, sections were washed in TBS and then treated with the secondary antibody, biotinylated horse anti-mouse IgG (1:200; Vector, BA2001), for 1 h. The reaction was amplified with streptavidin–biotin-peroxidase complex (1:300; DAKO, P0387) and visualized with 3,3-diaminobenzidine tetrahydrochloride (DAB; Sigma, D-5637). All sections were counterstained by cresyl fast violet and examined under the light microscope (Zeiss, Axiophot). For double labeling, mounted sections were blocked in TBS containing 10% normal goat serum (NGS) for 1 h, and then incubated with the first primary antibody: mouse anti-rat OX-6 (1:100; Serotec, MCA46R) or mouse anti-rat ED-1 (1:100; Serotec, MCA341R) IgG overnight, followed by a dilution (1:200) of fluorescein isothiocyanate (FITC)-conjugated goat anti-mouse IgG (Jackson ImmunoResearch, 115-095-100) or tetramethylrhodamine isothiocyanate (TRITC)-conjugated goat anti-mouse IgG (Jackson ImmunoResearch, 115-025-166) in TBS for 2 h. After washing, the section was treated with one of the second primary antibodies: mouse anti-rat CD11b IgG-conjugated *R*-phycoerythrin (RPE) (1:20; Serotec, MCA275PE) or biotinylated mouse anti-rat CD11b IgG (1:50; Serotec, MCA275B) overnight. The later antibody was then detected with dichlorotriazinylaminofluorescein (DTAF)-conjugated streptavidin (Jackson ImmunoResearch, 016-010-084) in TBS for 2 h. These sections were then counterstained by TOTO-3 iodide (1:5000, Molecular Probes, T3604), and then examined under a confocal laser scanning microscope (Zeiss, LSM510, Carl Zeiss, Germany) or fluorescence light microscope (Zeiss, Axiophot, Carl Zeiss, Germany).

2.3. Fluoro-Jade B (FJB) staining

FJB staining is well-established method to mark degenerating neurons and fibers (Schmued et al., 1997). Mounted sections were first immersed in a solution containing 1% sodium hydroxide in 80% alcohol for 5 min, followed by 70% alcohol and distilled water each for 2 min. The sections were then transferred to a solution of 0.06% potassium permanganate for 20 min, and rinsed several times in distilled water. The staining solution was prepared from a 0.01% stock solution of FJB (Chemicon, AG310) that was made by adding 10 mg of the dye powder to 100 ml of distilled water. To make up 100 ml of working solution, 4 ml of the stock solution was added to 96 ml of 0.1% acetic acid vehicle, resulting in a final dye concentration of 0.0004%. After 20 min incubation in the working solution, the sections were washed several times in distilled water each for 5 min, and examined in a fluorescence light microscope using green light (500–570 nm) excitation.

2.4. Immunoelectron microscopy

Eight rats were used for immunoelectron microscopy. The experimental animals were subjected to a similar process as mentioned above and sacrificed by perfusing with 4% paraformaldehyde at 1 and 3 days after KA injection. Following perfusion, the eye-cups were carefully dissected and immersed in 10% sucrose solution and kept in the same solution overnight at 4 °C. By a vibratome, the retina was cut sagittally into serial 100 μm thick sections. These floating sections were rinsed several times in 0.1 M PB, and then treated in a solution containing 1% hydrogen peroxide in TBS for 1 h. Sections were blocked for 1 h in a combination of 0.01% Triton X-100 and 10% NHS. They were then incubated overnight with the monoclonal antibody OX-42 (1:100; Serotec, MCA275R). After incubation, sections were washed in TBS, and then treated with the secondary antibody, biotinylated horse anti-mouse IgG (1:200; Vector, BA2001) for 1 h. The reaction was amplified with streptavidin–biotin-peroxidase complex (1:300; DAKO, P0387), and visualized with DAB (Sigma, D-5637). The brown-colored sections were post-fixed in 1% OsO_4 for 30 min. After osmication, floating sections were briefly rinsed in PB twice, and then dehydrated in an ascending series of ethanol. After dehydration, all specimens were embedded in pure Epon–Araldite mixture. Ultra-thin sections of the retina were double-stained with uranyl acetate and lead citrate. The stained sections were examined in a JOEL-2000 electron microscope.

Other four adult rats received intravitreal injection of 5 nM in a volume of 1.4 μl KA mixed with 1 μl of 1% horseradish peroxidase (HRP, type VI–A; Sigma, T6782). The experimental animals were sacrificed at 3 days after injection then perfused with 2% paraformaldehyde mixed with 2.5% glutaraldehyde in 0.1 M PB. Using a vibratome, the retina was cut sagittally into serial 100 μm thick sections for HRP reaction and electron microscopy preparation.

2.5. Quantitative study and statistical analysis

In the present study, the intensity of different labeled profiles was not estimated, instead of their total area and density being analyzed. Immunolabeled sections from the above-mentioned groups were used for enumeration of labeled profiles (three animals for each group). Three sections through the level of the optic disc from one retina of each rat were collected. A total of three images from the area about 1 mm width around the optic disc in three sections per retina for the respective immunostaining (OX-42, OX-6 and ED-1) were scrutinized using a light microscope at the magnification of 400×. The values of the total area of labeled profiles were obtained from the image analyzer (Image-Pro Plus) that defined the sum of gray-level pixels selected at a fixed threshold as the total area of labeled profiles. The constant threshold would be selected to cover all profiles of positive immunolabeling and applied to all grayscale digital images from sections with the same immunostaining. Because of a significant loss of retinal tissues starting at 3 days post-injection, the alterations of each immunomolecule in the atrophy retinas may not be reflected enough by the changes of the total area of labeled profiles. Therefore, the density of labeled profiles defined by the total area of labeled profiles against the area of the retinal profiles analyzed would be considered and may provide more information in understanding the revolution of immunomolecules in KA-challenged retinas. The area of the retinal profiles excluding the ONL and photoreceptor layer in each image captured was then measured and concomitantly the total area of labeled profiles was obtained from the same area. The areas of the retinal tissues at different time intervals were compared in a unit length (mm) of the retinal section. All data were expressed as mean ± S.E.M. in this study. Comparison of the total area of labeled profiles and the density of labeled profiles at various time points among groups was first analyzed using one-way ANOVA. At a fixed time point, differences between control and KA groups were analyzed using Student's *t*-test. Statistical difference was considered significant if $p < 0.05$.

3. Results

When compared with that of untreated/normal rats (data not shown), the retinas in rats receiving saline injection and killed at 1, 3, 7, 14 and 28 days appeared structurally normal (Figs. 1A, 2A and 3A). Although the retinal morphology at 1 day post-injection with KA was comparable to that in the saline-treated rats, many neurons at the inner border of the INL showed a pyknotic nucleus (Figs. 1B, 2B and 3B). A similar topography of degenerating profiles was revealed by FJB staining that also showed some degenerated cells at the GCL (Fig. 1C). At 3 days post-injection with KA, the NFL, GCL and IPL began to show signs of shrinkage with occasional pyknotic neurons. At 7, 14 and 28 days, the attenuated NFL, GCL and IPL collectively referred to as ANGI were hardly discernible.

3.1. Immunohistochemistry

3.1.1. OX-42 immunostaining

At different time intervals after saline injection (Fig. 1A), OX-42 positive microglial cells showed a similar distribution pattern in the NFL, GCL and IPL to the untreated/normal retinas (data not shown). At 1 day following KA injection, OX-42 labeled microglia/macrophages were noticeably hypertrophied but remained ramified. Furthermore, the immunoreactivity and profiles of cells especially those in the NFL, GCL and IPL were markedly enhanced when compared with those in the control retinas (Fig. 1B). At 3 days, many heavily stained cells were localized in the ANGI, INL and OPL, notably in areas adjacent to the inner border of the INL (Fig. 1D). At 7 days, microglia/macrophages exhibited the strongest OX-42 immunoreactivity and were distributed in the innermost retina (Fig. 1E). Interestingly, a variable number of OX-42 positive cells occurred between the outer segment of photoreceptor layer (OSPRL) and the pigmented epithelium (Fig. 1H), and remained populated in the ANGI (Fig. 1F,G) and the OSPRL (Fig. 1I and J) at 14 and 28 days post-injection. By quantitative analysis, labeled profiles of saline-treated retinas at all time intervals examined were comparable to those of the untreated/normal ones (data not shown). However, when compared with that in the controls, the total area of OX-42 immunoreactive profiles across all layers of the retina showed a drastic increase after KA injection. The upsurge reached its peak at 7 days, and after this, the value declined drastically till 28 days (Fig. 1K). In view of the significant loss of retinal tissue from 3 days after KA injection (Fig. 1L), the density (total area of labeled profiles/tissue area) of immunolabeled profiles with different antibodies was further estimated. The results confirmed that the increase in different immunolabeled profiles peaked at 7 days. In parallel to the total area of OX-42 immunoreactive profiles, the density of labeled profiles also showed a marked increase during the first week after KA injection; thereafter it declined drastically (Fig. 1M).

3.1.2. OX-6 immunostaining

OX-6 immunoreactive cells were undetected in the untreated/normal (data not shown) and saline-treated retinas at all time intervals (Fig. 2A). At 1 day after KA injection, OX-6 immunoreactive cells were ramified and detected in the NFL, GCL and IPL (Fig. 2B). At 3 days, many heavily labeled cells were observed with the majority of them in the ANGI, and most of them were rounded or emitted stout processes (Fig. 2C). At 7 days, OX-6 positive cells in the ANGI displayed an intense immunoreactivity and were concentrated at the inner margin of the ANGI and sporadically at the OSPRL (Fig. 2D and G). This was also true for OX-6 labeled cells at 14 (Fig. 2E and H) and 28 days (Fig. 2F and I), but the cell populations were markedly reduced when compared with earlier time intervals. Our quantitative study showed that the total area of OX-6 labeled profiles peaked at 3 days after KA injection and declined from 14 days onwards (Fig. 2J). On the other hand, the density of OX-6 immunoreactive profiles showed a gradual increase during the first 3 days after KA treatment. It peaked at 7 days and decreased gradually from 14 days onwards (Fig. 2K).

3.1.3. ED-1 immunostaining

Except for some ED-1 labeled cells in the choroid, labeled cells were not observed in the untreated/normal (data not shown) and saline-treated retinas at all time intervals examined (Fig. 3A). At 1 day after KA injection, punctuate ED-1 immunoreactive products were confined to labeled cells in the NFL and GCL (Fig. 3B). At 3 days, ED-1 positive cells

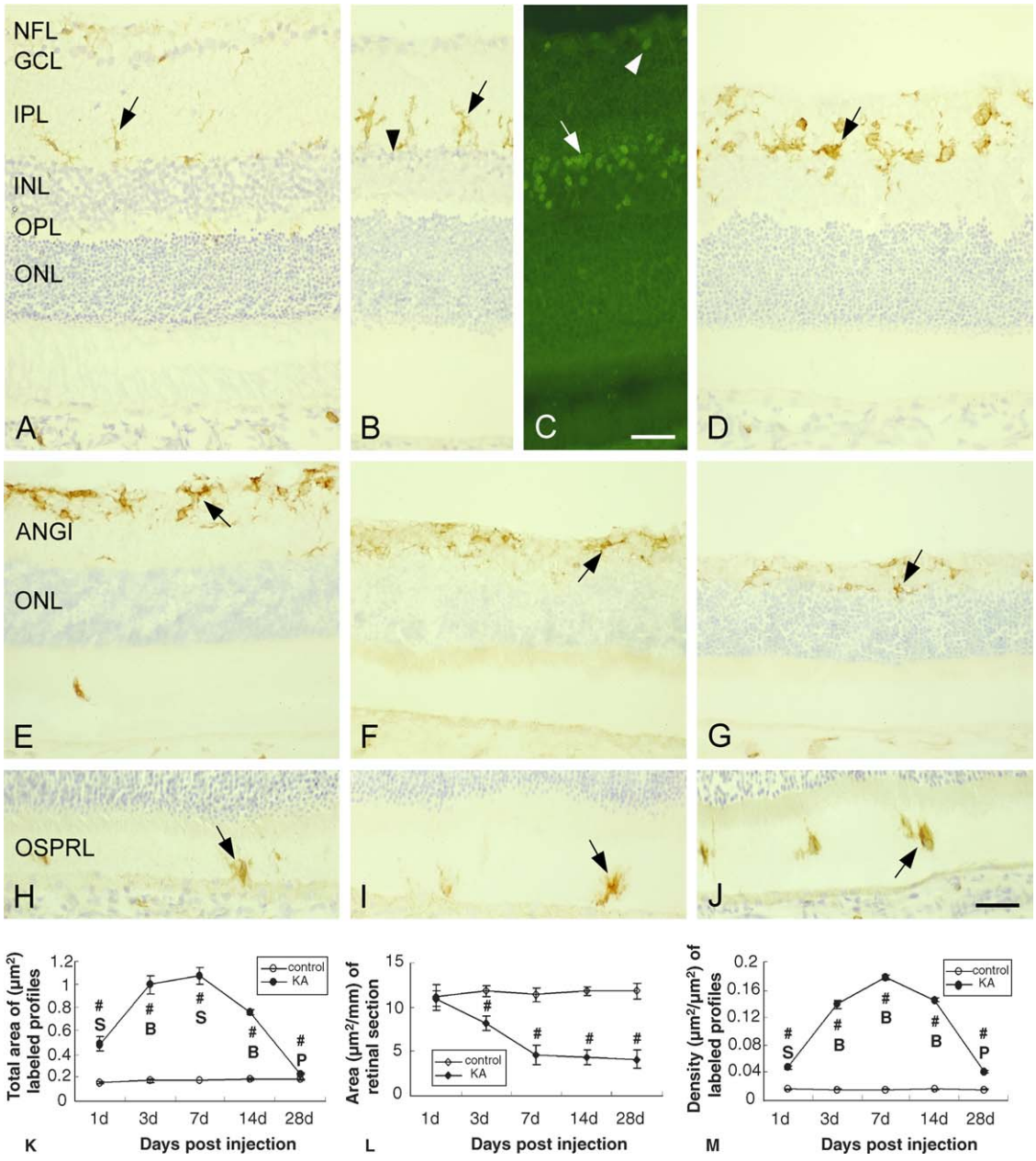

Fig. 1. OX-42 immunoreactivity in the retinas following saline (A) and kainate (B–I) injection. In rats receiving saline injection, OX-42 immunoreactivity is distributed in the NFL, GCL and IPL at various time points (A, arrow). One day following kainate injection, OX-42 immunoreactivity is enhanced (B, arrow). Meanwhile, many neurons showing pyknotic nuclei appear at the inner border of the INL (B, arrowhead) and are labeled by Fluoro-Jade B (FJB) staining (C, arrow). Note other FJB-positive neurons at the GCL (C, arrowhead). At 3 days, cells intensely stained for OX-42 are observed in the region adjacent to the inner border of the INL (D, arrow) and, at 7 days in the inner ANGI (E, arrow). OX-42 immunoreactive cells persist in the ANGI at 14 (F, arrow) and 28 (G, arrow) days. Note that a few OX-42 positive cells occur occasionally in the OSPRL at 7 (H), 14 (I) and 28 (J) days post-injection (arrows). Quantitative analysis shows that the total area of OX-42 immunoreactive profiles is significantly elevated at 1 day after kainate injection, peaked at 7 days but declined drastically thereafter (K). Note the considerable loss of retinal tissue beginning at 3 days till 7 days after kainate injection; subsequently the value being to plateau till 28 days (L). The density of OX-42 labeled profiles reaches its peak rapidly at 7 days after kainate injection and then declines drastically in the same manner (M). #, significant difference ($p < 0.05$) when compared with the saline-treated groups; P, significant difference ($p < 0.05$) when compared with the preceding time interval; S, significant difference ($p < 0.05$) when compared with the subsequent time interval; B, significant difference ($p < 0.05$) when compared with both the preceding and subsequent time intervals. NFL, nerve fiber layer; GCL, ganglion cell layer; IPL, inner plexiform layer; INL, inner nuclear layer; OPL, outer plexiform layer; ONL, outer nuclear layer; ANGI, attenuated NFL, GCL and IPL; OSPRL, outer segment of photoreceptor layer; scale bars = 50 μm.

appeared round or pleomorphic with some cells showing thin and stout processes, and were distributed in the ANGI, INL and OPL, more frequently at the junction between the ANGI and INL (Fig. 3C). ED-1 immunoreactive cells were sparsely distributed at 7 days and they tended to populate at the inner half of the ANGI (Fig. 3D). This distribution pattern of ED-1 positive cells was also observed at 14 (Fig. 3E) and 28 (Fig. 3F) days post-injection. As with OX-42 and OX-6 immunoreactive

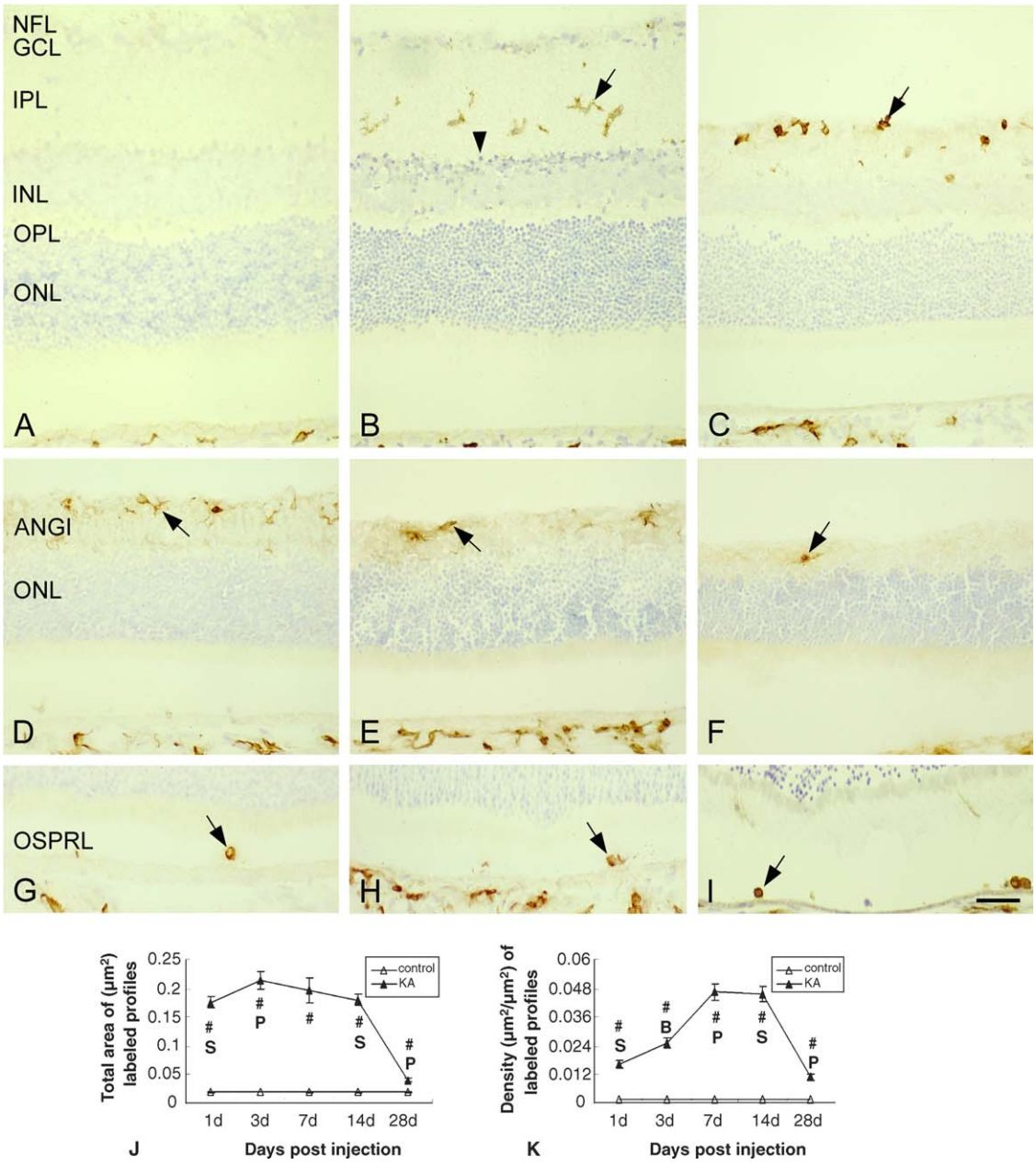

Fig. 2. OX-6 immunoreactivity in the retinas following saline (A) and kainate (B–I) injection. OX-6 immunoreactivity is absent in the saline-treated retina (A). At 1 day after kainate injection, OX-6 immunoreactivity (B, arrow) is markedly induced in ramified cells at the NFL, GCL and IPL with the occurrence of pyknotic nuclei (B, arrowhead) in the inner border of the INL. At 3 days, most of the OX-6 immunoreactive cells are round with some bearing stout processes (C, arrow). The distribution of OX-6 positive cells including those in OSPRL parallels that of OX-42 cells at 7 days (D and G, arrows). OX-6 immunoreactive cells persist at 14 (E and H, arrows) and 28 (F and I, arrows) days post-injection. By quantitative analysis, the total area of OX-6 labeled profiles (J) peaks at 3 days and declines steadily till 28 days. Note that the density of OX-6 labeled profiles (K) rises gradually in the initial stage, and decreases gradually after peaking at 7 days. Abbreviations and symbols same as in Fig. 1; scale bar = 50 μm.

cells, a variable number of ED-1 positive cells were observed at the OSPRL at different time intervals (Fig. 3G–I). Similar to those of OX-6 immunoreactive profiles, quantitative analysis indicated a peak total area of ED-1 labeled profiles at 3 days after KA injection and a steady decrease thereafter (Fig. 3J). It is also true for the density of ED-1 immunoreactive profiles that showed a gradual increase at beginning of injury after KA treatment following by a climax at 7 days and a gradual reduction from 14 days onwards (Fig. 3K).

3.1.4. Immunophenotypes of microglia/macrophages in KA-challenged retinas

In order to get insight into the nature of microglia/macrophages in KA-challenged retinas, double labeling of the abovementioned immunomolecules was applied. We found that cells concurrently expressing CR3 and unknown cytoplasmic/lysosomal antigens ($OX\text{-}42^{+}/ED\text{-}1^{+}$, Fig. 4A–C) existed mainly in the inner retinas and remained ramified at the first 3 days post-injection. At the same period of KA

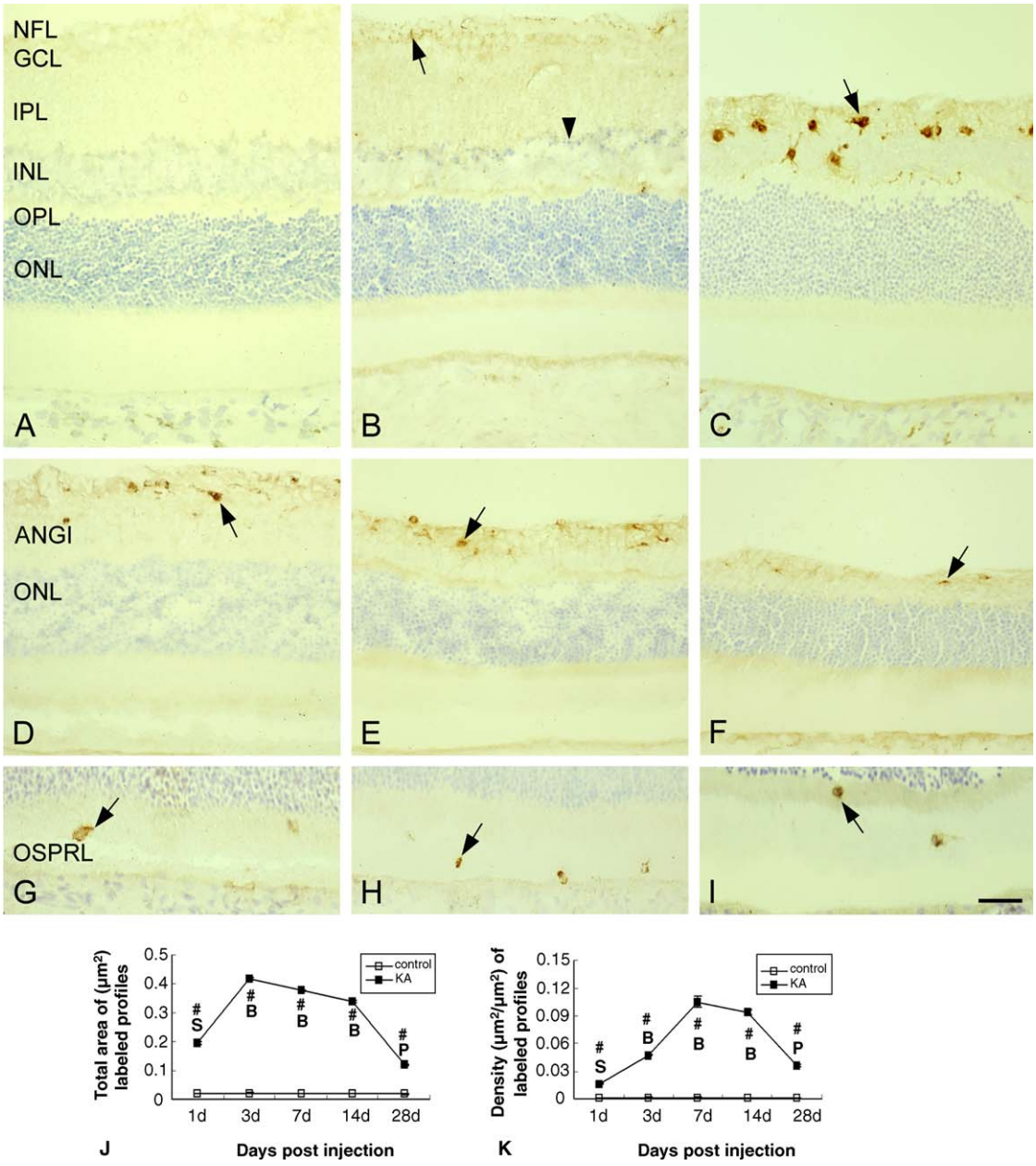

Fig. 3. ED-1 immunoreactivity in the retinas following saline (A) and kainate (B–I) injection. ED-1 immunoreactivity is undetected in saline-injected rats (A). At 1 day after kainate injection, punctate ED-1 immunoreaction products (B, arrow) are induced mainly in the NFL with concurrent occurrence of a few pyknotic nuclei at the inner border of the INL (B, arrowhead). At 3 days, round ED-1 positive cells with some of them showing thin and stout processes (C, arrow) appear in vicinity of the inner INL. As with OX-42 and OX-6 immunoreactive cells, ED-1 immunoreactive cells appear to populate at the inner half of the ANGI and occasionally in the OSPRL at 7 (D and G, arrows) 14 (E and H, arrows) and 28 (F and I, arrows) days. Similar to the expression pattern of OX-6 labeled profiles, the total area of ED-1 labeled profiles (J) also peaks at 3 days and declines steadily till 28 days. Quantitative data further show a gradual increase of the density of ED-1 labeled profiles (K) in the initial stage of kainate stimulation and a steady decrease after its peak expression at 7 days. Abbreviations and symbols same as in Fig. 1; scale bar = 50 μm.

challenge, other ramified cells expressing CR3 also contained MHC class II molecules (OX-42$^+$/OX-6$^+$, Fig. 5A–C) and occurred frequently at the NFL and GCL.

3.2. Electron microscopic study

By immunoelectron microscopy, OX-42 positive cells in the untreated/normal retinas showed immunoreaction product at the plasma membrane and displayed characteristic features of microglia (Fig. 6A). At 1 day after KA injection, OX-42 labeled microglia showed more abundant cytoplasm containing numerous OX-42 positive vesicles and a few lysosomes and phagosomes (Fig. 6B). Meanwhile, degenerating neurons found at the inner border of the INL showed a pyknotic nucleus containing irregular clump of electron-dense chromatin and disorganized cytoplasm with some vacuoles and swollen mitochondria (Fig. 7A). Cell processes either positive or negative for OX-42 frequently surrounded the degenerating cells (Fig. 7A and B). Similar degenerating neurons (Fig. 7B) were observed at 3 days when OX-42 labeled microglia/

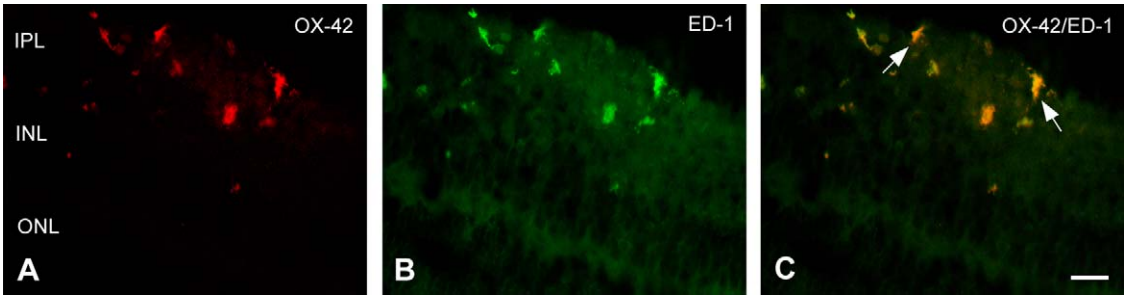

Fig. 4. Fluorescent images of retinal microglia/macrophages double-labeled with OX-42 (A) and ED-1 (B) at 3 days after kainate injection. Microglia/macrophages in kainate-challenged retinas are labeled with anti-OX-42 IgG-conjugated RPE (A, red) followed by anti-ED-1 antibody visualized with goat anti-mouse IgG-conjugated FITC (B, green). The merged image (C) shows that microglia/macrophages in lesioned retinas concurrently express OX-42 and ED-1 immunoreactivities (C, yellow) and are ramified in form (C, arrows). Abbreviations same as in Fig. 1; scale bar = 50 μm.

macrophages were characterized by their copious cytoplasm endowed with immunoreactive vesicles and phagosomes (Fig. 8A). Some labeled cells were rounded or amoeboidic with an indented nucleus. Its moderate amount of cytoplasm contained OX-42 labeled vesicles, tubule-like structures and vacuoles (Fig. 8B). In addition, many microglia/macrophages were laden with lipid droplets and phagosomes containing reaction products of exogenous HRP that was co-administrated with KA into the vitreum (Fig. 9A and B). Occasionally HRP products were also found in lysosome-like structures of other cells resembling Müller cells or astrocytes. The latter cells also appeared to enclose degenerating debris (Fig. 9A–C).

4. Discussion

In optic nerve axotomy model, Garcia-Valenzuela et al. (2005) detected an alteration of OX-42 labeled microglial cells in the affected retinas at day 5 after lesioning. The number of reactive microglia in the GCL appeared to reach its peak at day 12 post-lesion. Using fluorescent microspheres to label circulating monocytes, the authors concluded a limited contribution of blood borne macrophages in the axotomized retinas (Garcia-Valenzuela and Sharma, 1999; Garcia-Valenzuela et al., 2005). In the same injury model, Zhang and Tso (2003) also demonstrated that OX-42 positive cells in the inner retina could phagocytose dying ganglion cells and migrate to the subretinal space. It was suggested that OX-42 and ED-1 positive cells in the normal and lesioned retinas were resident microglia. In retinal ischemia/reperfusion injury, Zhang et al. (2005) reported the occurrence of numerous intensely labeled OX-42, ED-1 and OX-6 cells in the inner retina early at 1 day after ischemia and the distribution of labeled cells in the subretinal space during 3–14 days of recovery. Using RCA-1 histochemistry to label phagocytes, Shin et al. (2000) stated that microglia were the only phagocytes involved in clearance of apoptotic debris from the inner retinas at 1 day after kainate injection. We confirm here an early response of OX-42, ED-1 and OX-6 labeled cells in the inner retina at 1 day after kainate injection and, furthermore, a significant distribution of them in the OSPRL (subretinal space) during the late stage of excitotoxic injury. It would appear therefore from studies by others as well as by us that the rapid reactive response of microglia to retinal injury is a general phenomenon. The present ultrastructural results however have added the fact that the retinal Müller cells other than microglia/macrophages also partake in the removal of cellular debris induced by kainate.

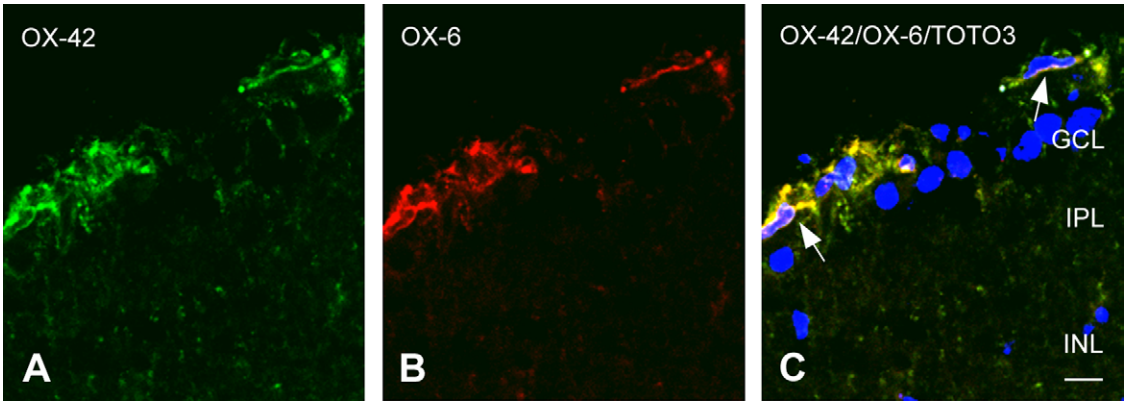

Fig. 5. Confocal images of retinal microglia/macrophages double-labeled with OX-42 (A) and OX-6 (B) at 3 days after kainate injection. Retinal microglia/macrophages are subjected to mark with biotinylated anti-OX-42 antibody detected with streptavidin-conjugated DTAF (A, green) and subsequently with anti-OX-6 antibody imagined with goat anti-mouse IgG-conjugated TRITC (B, red). In the merged image (C) with TOTO-3 nuclear staining (blue), it demonstrates the co-expression (yellow) of OX-42 and OX-6 immunoreactivities on microglia/macrophages that still bear cell processes (C, arrows). Abbreviations same as in Fig. 1; scale bar = 50 μm.

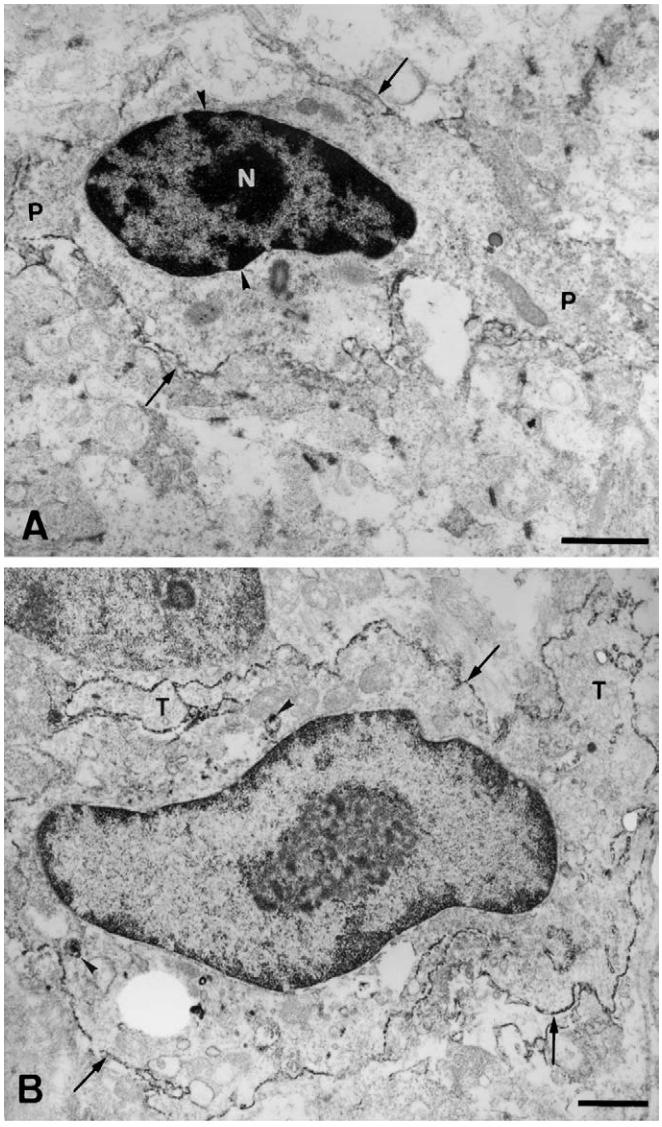

Fig. 6. Electron micrographs showing OX-42 immunoreactive cells in the normal rat retina (A) and at 1 day post-injection with kainate (B). The cell in the normal retina shows OX-42 immunoreactivity at its plasma membrane (A, arrows) and emits processes (A and P). Its nucleus (N) is small and irregular and bears heterochromatin masses (A, arrowheads) beneath the nuclear envelope. OX-42 positive cell (B) at 1 day after kainate injection displays a rod-shaped soma that contains more abundant cytoplasm and emits numerous thinner processes (B and T). The OX-42 immunoreactivity is increased at its plasma membrane (B, arrows) and vesicles (B, arrowheads); scale bars = 1 μm.

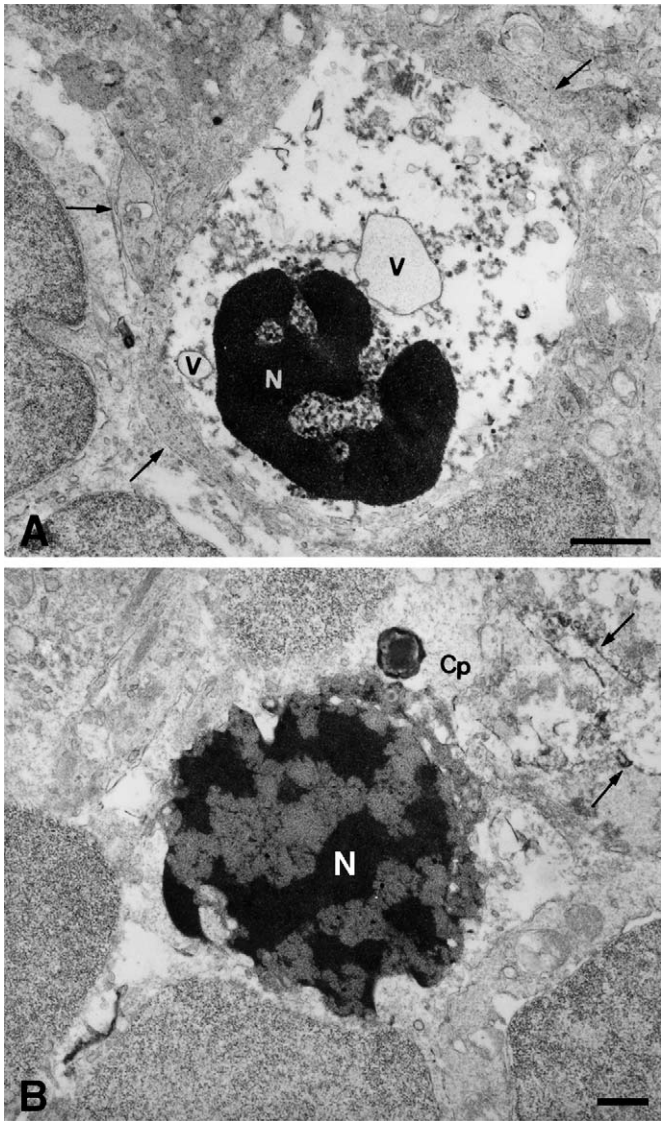

Fig. 7. Electron micrographs of degenerating neurons in the retinas at 1 (A) and 3 days (B) after kainate injection. At 1 day, the degenerating neuron in the inner border of the INL (A) undergoes necrosis with a pyknotic nucleus (A and N) and disrupted cytoplasm with vacuoles (A and V). Arrows in (A) indicate OX-42 negative cytoplasmic processes that appear to surround the degenerating neuron. At 3 days, a degenerating neuron (B) showing disintegrated nucleus (B and N) and cytoplasm (B and Cp) is in close apposition to an OX-42 labeled cytoplasmic process (B, arrows); scale bars = 1 μm.

Our quantitative study has further demonstrated a distinct expression pattern between OX-42 and ED-1/OX-6 immunoreactivities (not numbers of OX-42, ED1 and OX-6 labeled cells) in lesioned retinas suggesting that this may be a differential or specific response of subsets of retinal microglia/macrophages to kainate stimulation.

In untreated or control retinas, microglia bearing CR3 were widely distributed across the different layers of retina, which were devoid of MHC class II and ED-1 unknown cytoplasmic/lysosomal antigens. Following kainate injection, CR3 immunoreactivity of cells especially those in the NFL, GCL and IPL was markedly enhanced. Furthermore, the cells were clearly hypertrophied when compared with those in the control retinas. Moreover, the present study has shown that kainate induced the expression of MHC class II and ED-1 antigens in retinal ramified cells coincident to those labeled by CR3 antibody in terms of their spatial distribution and colocalization of immunomolecules. The characteristic immunophenotypes of retinal microglia have been reported in different injury or disease models of the retina (Leon et al., 2000; Zeng et al., 2000; Fauser et al., 2001). For example, in the diabetic retina (Zeng et al., 2000) or the retina of experimental autoimmune uveitis (Fauser et al., 2001), microglia were activated to express MHC class II and ED-1 antigens that were increased across the

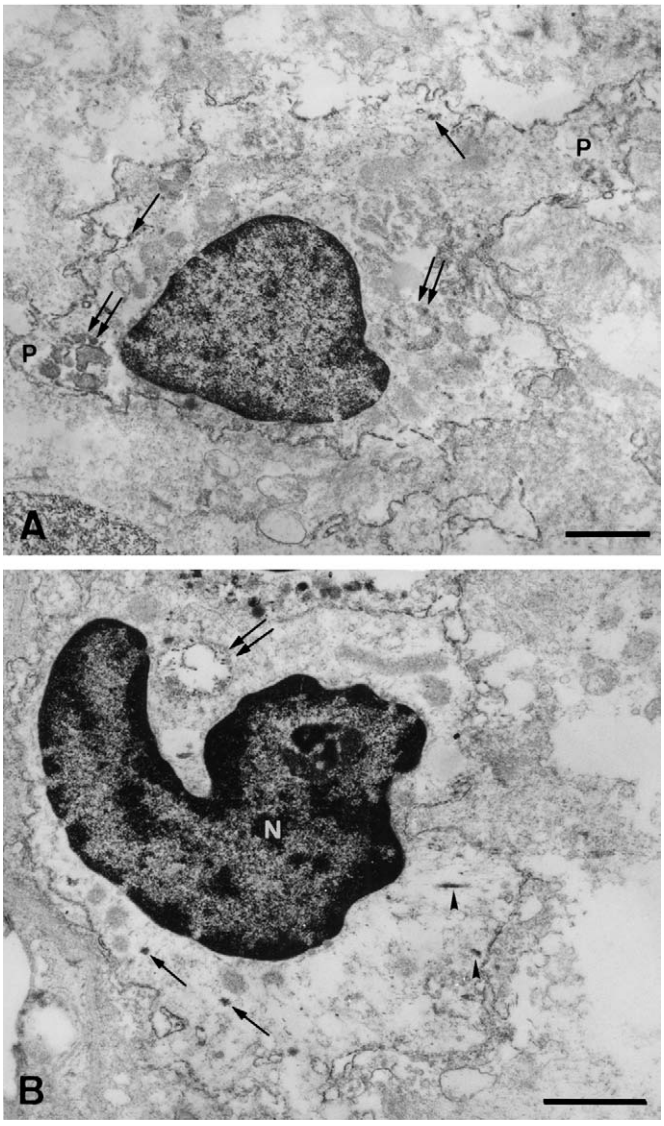

Fig. 8. Electron micrographs of OX-42 positive cells in the retina at 3 days after kainate injection. OX-42 immunoreactive cells at 3 days are amoeboidic (A) or rounded (B) in outline. The immunoreactive cell in (A) shows broad processes (P) and abundant cytoplasm containing vesicles (A, arrows) and phagosomes (A, double arrows) with OX-42 immunoreaction products. The round immunoreactive cell (B) has an indented nucleus (N) and moderate amount of cytoplasm. Its vesicles (B, arrows), tubule-like structures (B, arrowheads) and vacuoles (B, double arrows) are positive for OX-42; scale bars = 1 μm.

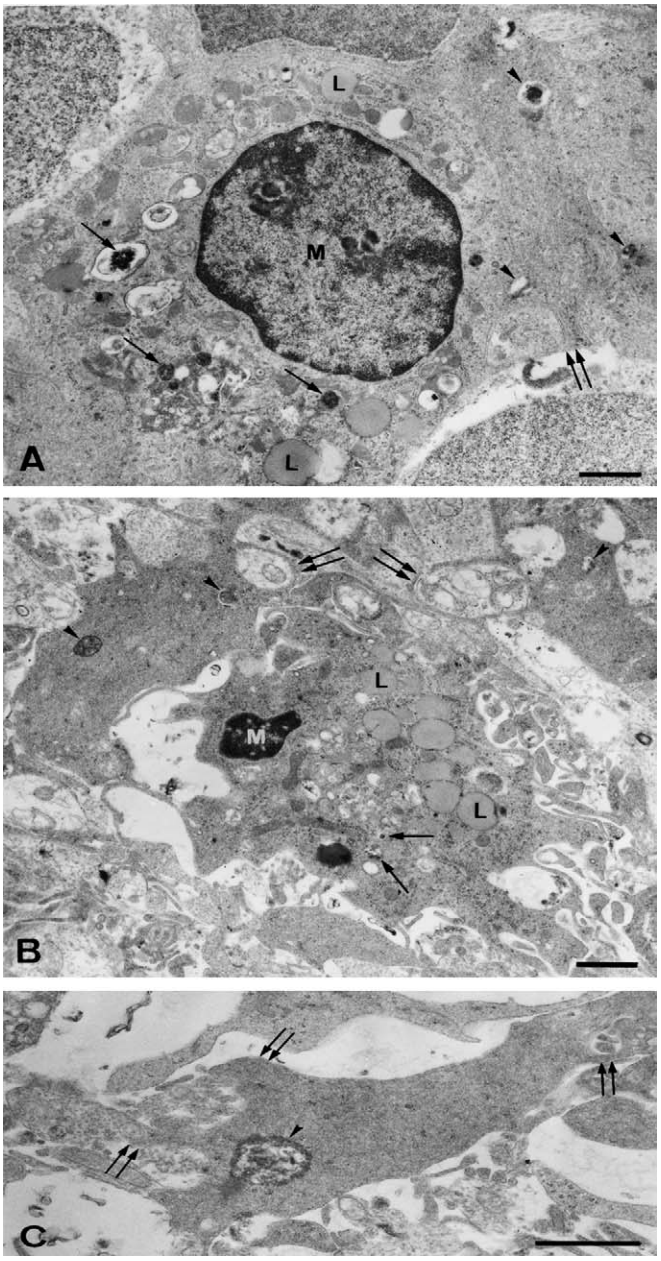

Fig. 9. Electron micrographs of the retinal structures at 3 days after co-injection with kainate and HRP. Note full-blown microglia/macrophages (A and B, M) possessing numerous lipid droplets (A and B, L) and phagosomes incorporating HRP reaction products (A and B, arrows). Near to the above cells are cell processes that show a slightly darker cytoplasm resembling Müller cells or astrocytes. These processes also include HRP reaction products in lysosome-like structures (A–C, arrowheads) and appear to surround some degenerating tissues (B and C, double arrows); scale bars = 1 μm.

different retinal layers and extended into the ONL at later period of the disease (Zeng et al., 2000). An increased level of cells positive for ED-1 in the retina by lens injury or by intraocular injection of a macrophage activator (Zymosan) had been further demonstrated (Leon et al., 2000). The induction of MHC class II and ED-1 antigens may therefore reflect a common signal of microglial activation in the affected retina and function in antigen presentation, sampling/cleaning endogenous and exogenous intraocular molecules and/or probably promoting tissue regeneration (Leon et al., 2000).

By quantitative analysis, we have shown that the total area of labeled profiles of either MHC class II or ED-1 antigens in retinal microglia/macrophages peaked at 3 days after kainate injection. The density of the labeled profiles, however, reached its peak at 7 days. This may be attributed to the severe loss of retinal tissues at 7 days. Both the density and total area of CR3 immunoreactive profiles were coincident peaking at 7 days and they decreased drastically thereafter. In contrast, the retinal microglia/macrophages expressing either MHC class II or ED-1 antigens showed a slow decline after peaking at 3 and 7 days in the total area and density of labeled profiles, respectively, at the later time intervals. The significance of differential

expressions of CR3 and MHC class II/ED-1 antigens in microglia/macrophages following injection is unclear. This may hypothetically be attributed to the constitutive and inducible nature of CR3 and MHC class II/ED-1 antigens, respectively, in retinal microglia that demanded these immunomolecules differentially in response to tissue injury. A noteworthy feature in this study was that cells expressing the respective or two immunomolecules remained ramified at 1–3 days after kainate injection. At 3 days, however, more round and amoeboid microglia/macrophages were observed. It is suggested that the round and amoeboidic microglia/macrophages are derived from activation and transformation from the ramified microglial cells. The possibility of invasion of circulating monocytes giving rise to these cells at later time points cannot be excluded.

It is well documented that microglial cells are pathologic sensor as they respond vigorously and swiftly to subtle changes in their ambient environment (Wu et al., 1997; Ling et al., 2001; Chang et al., 2003). A novel finding in the present study was the increase in immunomolecules of microglia/macrophages in the inner border of the INL in kainate-treated rats especially in those killed at 3 days. The robust microglia/macrophages reaction in the inner border of the INL is consistent with previous results by Morgan and Ingham (1981), who showed that low doses (6 nM) of kainate significantly produced lesion confined to the IPL and INL where amacrine cells were markedly reduced in number. It is therefore speculated that microglia/macrophages reaction in lesioned retina may be elicited by kainate-induced amacrine cell deaths that are concentrated at the inner border of the INL. Previous studies have also shown that optic axotomy significantly caused ganglion cell death in the GCL and induced microglial population changes in the restricted layer such as the NFL, GCL or IPL (Zhang and Tso, 2003). This is in agreement with our present results showing an increased immunomolecules of microglia/macrophages adjacent to the vitreal surface of kainate-treated retina at later time periods. It is noteworthy that the main retinal vasculatures are distributed in the same region. Perivascular accumulation of microglia/macrophages has been evidenced during the later stages of various brain injuries or diseases (Wu et al., 1997; Grossmann et al., 2002). In this connection, we proposed that retinal microglia/macrophages accumulation in the inner ANGI may be recruited toward the blood vessels at later time points of kainate-induced injuries. An interesting feature in the kainate-treated retina was the occurrence of some OX-42, OX-6 and ED-1 labeled microglia/macrophages in the region between the OSPRL and the retinal pigment epithelium at various time intervals a feature that was reported by Shin et al. (2000) who also examined microglial reaction in the retina after application with kainate. It has been reported that kainite-induced degenerative changes in other brain tissues were accompanied by monocyte invasion from blood circulation (Sola et al., 1997). In diabetic retina, neuronal degeneration was accompanied by microglial migration either from resident microglia in the NFL and GCL or infiltration of monocytes from the retinal blood vessels (Zeng et al., 2000). In the present study, labeled cells in the OSPRL may be derived from the circulating monocytes in the vessel-rich choroid. Indeed, in the study on photocoagulated rabbit retina it was reported that monocytes invaded the retina from the choroid through the Bruch's membrane (Ishikawa et al., 1983).

Previous studies have shown that phagocytes can be induced under a variety of microenvironmental disturbances in the retina. Microglia, which eliminate the degenerating debris from the central nervous system (Shin et al., 2000) thus functioning as phagocytes, have also been regarded as important immune effector cells in the retina (Zeng et al., 2000). Recently, Shin et al. (2000) have suggested that microglial cells are likely to be the one and only type of phagocytes in the kainate-induced retinal apoptosis. Besides phagocytes, Müller cells, the principal neuroglial cells in the retina (Newman and Reichenbach, 1996), are also involved in phagocytosis during the development (Egensperger et al., 1996) and in various pathologic conditions of the retina (Roque and Caldwell, 1990; Kim et al., 1998). Our immunoelectron microscopic study has shown that microglia/macrophages endowed with CR3 and which are known to be involved in phagocytosis contained a significant amount of phagosomes at 1 and 3 days after kainate-induced degeneration. The present ultrastructural examination further showed that cell elements other than microglia/macrophages particularly those resembling Müller cells or astrocytes frequently wrapped degenerating neurons or structures and contained exogenous HRP reaction products in their lysosome-like structures, indicating their phagocytic capability.

In conclusion, microglia/macrophages reaction, probably indicative of cell activation, is linked to neuronal cell loss/degeneration, both occurring between 1 and 28 days of kainate-induced excitotoxicity. On the other hand, the present results suggest that microglia/macrophages are not the only type of phagocytes in kainate-lesioned retina in rats. Their phagocytosis capacity may not be sufficient enough to eliminate kainate-induced degenerating debris that was removed by other retinal cells of non-phagocyte nature.

Acknowledgements

This study was supported in part by research grants (NSC 92-2320-B002-113 and NSC 93-2320-B002-033) from National Science Council, Taiwan.

References

Chang, C.Y., Chien, H.F., Jiangshieh, Y.F., Wu, C.H., 2003. Microglia in the olfactory bulb of rats during postnatal development and olfactory nerve injury with zinc sulfate: A lectin labeling and ultrastrucutural study. Neurosci. Res. 45, 325–333.

Dreyer, E.B., Zurakowski, D., Schumer, R.A., Podos, S.M., Lipton, S.A., 1996. Elevated glutamate levels in the vitreous body of humans and monkeys with glaucoma. Arch. Ophthalmol. 114, 299–305.

Dreyfus, H., Sahel, J., Heidinger, V., Mohand-Said, S., Guerold, B., Meuillet, E., Fontaine, V., Hicks, D., 1998. Gangliosides and neurotrophic growth factors in the retina: Molecular interactions and applications as neuroprotective agents. Ann. N. Y. Acad. Sci. 845, 240–252.

Egensperger, R., Maslim, J., Bisti, S., Hollander, H., Stone, J., 1996. Fate of DNA from retinal cells dying during development: uptake by microglia and macroglia (Müller cells). Brain Res. Dev. Brain Res. 97, 1–8.

Fauser, S., Nguyen, T.D., Bekure, K., Schluesener, H.J., Meyermann, R., 2001. Differential activation of microglial cells in local and remote areas of IRBP1169–1191-induced rat uveitis. Acta Neuropathol. 101, 565–571.

Garcia-Valenzuela, E., Sharma, S.C., 1999. Laminar restriction of retinal macrophagic response to optic nerve axotomy in the rats. J. Neurobiol. 40, 55–66.

Garcia-Valenzuela, E., Sharma, S.C., Pina, A.L., 2005. Multilayered retinal microglial response to optic nerve transaction in rats. Mol. Vis. 11, 225–231.

Grossmann, R., Stence, N., Carr, J., Fuller, L., Waite, M., Dailey, M.E., 2002. Juxtavascular microglia migrate along brain microvessels following activation during early postnatal development. Glia 37, 229–240.

Honjo, M., Tanihara, H., Kido, N., Inatani, M., Okazaki, K., Honda, Y., 2000. Expression of ciliary neurotrophic factor activated by retinal Müller cells in eyes with NMDA- and kainic acid-induced neuronal death. Invest. Ophthalmol. Vis. Sci. 41, 552–560.

Ishikawa, Y., Momoeda, S., Yoshitomi, F., 1983. Origin of macrophage in photocoagulated rabbit retina. Jpn. J. Ophthalmol. 27, 138–148.

Kim, I.B., Kim, K.Y., Joo, C.K., Lee, M.Y., Oh, S.J., Chung, J.W., Chun, M.H., 1998. Reaction of Müller cells after increased intraocular pressure in the rat retina. Exp. Brain Res. 121, 419–424.

Kleinschmidt, J., Zucker, C.L., Yazulla, S., 1986. Neurotoxic action of kainic acid in the isolated toad and goldfish retina: I. Description of effects. J. Comp. Neurol. 254, 184–195.

Leon, S., Yin, Y., Nguyen, J., Irwin, N., Benowitz, L.I., 2000. Lens injury stimulates axon regeneration in the mature rat optic nerve. J. Neurosci. 20, 4615–4626.

Ling, E.A., Ng, Y.K., Wu, C.H., Kaur, C., 2001. Microglia: its development and role as a neuropathology sensor. Prog. Brain Res. 132, 61–79.

Lopez-Colome, A.M., Ortega, A., Romo-de-Vivar, M., 1993. Excitatory amino acid-induced phosphoinositide hydrolysis in Müller glia. Glia 9, 127–135.

Matsubara, T., Pararajasegaram, G., Wu, G.S., Rao, N.A., 1999. Retinal microglia differentially express phenotypic markers of antigen-presenting cells in vitro. Invest. Ophthalmol. Vis. Sci. 40, 3186–3193.

Morgan, I.G., Ingham, C.A., 1981. Kainic acid affects both plexiform layers of chicken retina. Neurosci. Lett. 21, 275–280.

Newman, E., Reichenbach, A., 1996. The Müller cell: a functional element of the retina. Trends Neurosci. 19, 307–312.

Ogden, T.E., 1994. Glia. In: Stephen, J.R. (Ed.), Retina. Mosby, St. Louis, pp. 54–57.

Roque, R.S., Caldwell, R.B., 1990. Müller cell changes precede vascularization of the pigment epithelium in the dystrophic rat retina. Glia 3, 464–475.

Schmued, L.C., Albertson, C., Slikker Jr., W., 1997. Fluoro-Jade: a novel fluorochrome for the sensitive and reliable histochemical localization of neuronal degeneration. Brain Res. 751, 37–46.

Shin, D.H., Lee, H.Y., Lee, H.W., Lee, K.H., Lim, H.S., Jeon, G.S., Cho, S.S., Hwang, D.H., 2000. Activation of microglia in kainic acid induced rat retinal apoptosis. Neurosci. Lett. 292, 159–162.

Sola, C., Tusell, J.M., Serratosa, J., 1997. Calmodulin is expressed by reactive microglia in the hippocampus of kainic acid-treated mice. Neuroscience 81, 699–705.

Tamai, K., Toumoto, E., Majima, A., 1997. Local hypothermia protects the retina from ischemic injury in vitrectomy. Br. J. Ophthalmol. 81, 789–794.

Ulshafer, R.J., Sherry, D.M., Dawson, R., Wallace Jr., D.R., 1990. Excitatory amino acid involvement in retinal degeneration. Brain Res. 531, 350–354.

Vorwerk, C.K., Naskar, R., Schuettauf, F., Quinto, K., Zurakowski, D., Gochenauer, G., Robinson, M.B., Mackler, S.A., Dreyer, E.B., 2000. Depression of retinal glutamate transporter function leads to elevated intravitreal glutamate levels and ganglion cell death. Invest. Ophthalmol. Vis. Sci. 41, 3615–3621.

Wang, C.C., Wu, C.H., Shieh, J.Y., Wen, C.Y., Ling, E.A., 1996. Immunohistochemical study of amoeboid microglial cells in fetal rat brain. J. Anat. 189, 567–574.

Wu, C.H., Wang, H.J., Wen, C.Y., Lien, K.C., Ling, E.A., 1997. Response of amoeboid and ramified microglial cells to lipopolysaccharide injections in postnatal rats—a lectin and ultrastructural study. Neurosci. Res. 27, 133–141.

Zeevalk, G.D., Hyndman, A.G., Nicklas, W.J., 1989. Excitatory amino acid-induced toxicity in chick retina: amino acid release, histology, and effects of chloride channel blockers. J. Neurochem. 53, 1610–1619.

Zeng, X.X., Ng, Y.K., Ling, E.A., 2000. Neuronal and microglial response in the retina of streptozotocin-induced diabetic rats. Vis. Neurosci. 17, 463–471.

Zhang, C., Tso, M.O., 2003. Characterization of activated retinal microglia following optic axotomy. J. Neurosci. Res. 73, 840–845.

Zhang, C., Lam, T.T., Tso, M.O., 2005. Heterogeneous populations of microglia/macrophages in the retina and their activation after retinal ischemia and reperfusion injury. Exp. Eye Res. (Epub ahead of print).

Zhang, J., Wu, G.S., Ishimoto, S., Pararajasegaram, G., Rao, N.A., 1997. Expression of major histocompatibility complex molecules in rodent retina: Immunohistochemical study. Invest. Ophthalmol. Vis. Sci. 38, 1848–1857.